Microcontroller based electric field mill sensor interface

Alexandros Chatzis
Physics Department
Aristotle University of Thessaloniki
Thessaloniki, Greece
alekchat@physics.auth.gr

Zoi Agorastou
Electronics Lab, Physics Dept.
Aristotle University of Thessaloniki
Thessaloniki, Greece
zagorast@physics.auth.gr

Stylianos Siskos
Electronics Lab, Physics Dept.
Aristotle University of Thessaloniki
Thessaloniki, Greece
siskos@physics.auth.gr

***Abstract*—The measurement of electric field for applications where atmospheric/meteorological phenomena are examined, as well as in industry applications, provides a great amount of information regarding lightning incidents and safety margins. In this paper, the electric field mill sensor - the prominent sensor employed for electric field measurements - was studied, and an interface circuit was designed and successfully tested. More specifically, a two-stage amplification circuit was designed which was comprised of a charge amplifier for charge to voltage conversion and an inverting amplifier for further amplification and fine tuning. A low noise operational amplifier was selected and used so that the noise levels were kept at minimum levels. Differential measurements were also taken and compared to the single-ended measurements. An Arduino microcontroller was implemented to complete the interface and its operation was the extraction of the electric field values.**

Keywords*—*electric field mill, sensor interface, Arduino microcontroller

I. Introduction

The electric field in the atmosphere is directly proportional to the frequency of thunderstorms and lightning incidents, and furthermore it is indicative of the presence of aerosols, charged dust clouds and radioactive pollution in the air [1,2]. Therefore, the study of the number and the intensity of electric discharges in the atmosphere, as well as their polarity is of great significance. A sensor that can be employed to study lightning incidents, and furthermore to develop lightning warning systems is the electric field mill. In these lightning warning systems, a margin is set for the minimum electric field in the atmosphere prior triggering lightning. Atmospheric conditions such as humidity and dust particles play an important role on where that margin would be and for safety reasons, that margin is set much lower than the observed minimum in those systems. Another important part is that the quality of air and the atmospheric pollution are strongly related to the electric field, as observed in numerous studies [1]. In industry applications, where high electric fields are present, monitoring of the electric field level is necessary so that safety margins are observed, e.g., under high voltage dc power lines. Moreover, the increase of high voltage DC power transmission has brought the need of further investigations about the electric field values around these lines for safety, health, and research purposes [3, 4].

For this paper, the field mill sensor was studied and designed, so that it could be possible to inspect the function of the interface circuit in laboratory conditions. A system of measuring electric fields from -15 kV/m up to 15 kV/m is adequate, as for studying lightning incidents the minimum electric fields prior triggering lightning is about 6kV/m [5].

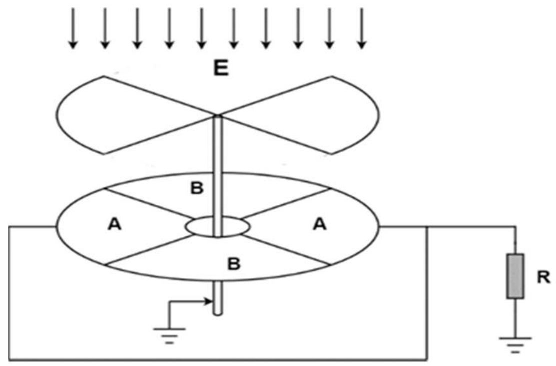

Fig. 1: The field mill sensor with a resistor

II. Principle of Operation of the Field Mill Sensor

The field mill sensor consists of a circular disk divided by conductive plates which are the sensing electrode with surface A and the sensing electrodes with surface B, as shown in Fig. 1. A grounded rotor rotates above the disk exposing and screening the sensor plates periodically with the help of a constant speed motor.

When the sensor is exposed to a static electric field, the exposed part of surface A varies linearly with time. From Gauss's Law, it is derived that the induced charge varies also linearly with time (1), where ε_0 is the vacuum permittivity and E is the electric field.

$$q = \varepsilon E A(t) \tag{1}$$

For constant electric field strength E, a square wave current will flow through resistor R, since the current $i(t)$ is given by:

$$i(t) = \frac{dq(t)}{dt} = \varepsilon_0 E \frac{dA(t)}{dt} \tag{2}$$

Equation (2) shows that the current $i(t)$ and the corresponding voltage $v_R(t)$ across resistor R is directly proportional to the incident electric field [5, 6].

In the present study, a field mill with four sensor plates connected as two sets and with two vanes attached to the grounded rotor was constructed. In every full rotation, each set of electrodes is shielded two times. As a result, the relation between the signal frequency ω and the rotational frequency is:

$$\omega = 2\omega' \tag{3}$$

979-8-3503-9958-5/22/$31.00 ©2022 IEEE

The output signal of the field mill sensor, given the rotational frequency and the surface of the sensor plates, is in the order of pico-Amperes to nano-Amperes in fair weather conditions. Consequently, the amplification of that signal is mandatory. That weak signal is in the order of magnitude of the noise that is introduced into the system so filtering the signal with a low pass filter is also important. To amplify that small signal the resistance R is substituted with the charge amplifier which is an opamp-based circuit using an RC network at the negative feedback (Fig. 2), whose operation is to convert the output charge of the sensor to voltage. Solving the circuit's differential equation for $0 \leq t < T/2$ results in an expression for the exponential output voltage *v(t)*.

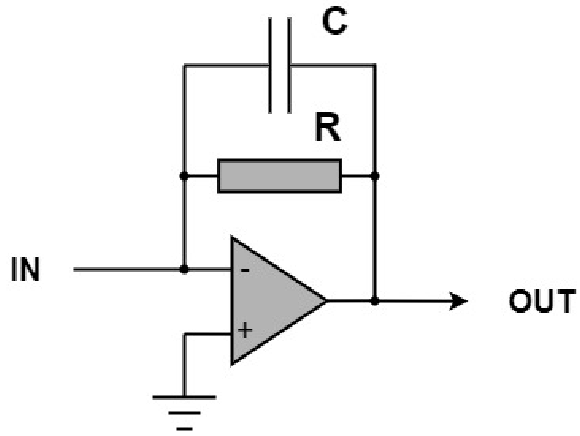

Fig. 2: Charge amplifier

By evaluating *v(t)* on *t=T/2*, the amplitude *V* is calculated:

$$V = \frac{\omega}{\pi} * \varepsilon_0 * A * E * R * tahn\left(\frac{\pi}{2\omega RC}\right) \tag{4}$$

According to (4), the amplitude of the signal is also dependent of the rotation speed of the rotor and small fluctuations of that speed can introduce changes in the signal amplitude. With the correct value of the RC impedance the product of ω and RC can be high enough for the amplitude V to become independent of the rotor speed, as shown in (6) [3, 6].

$$V = \frac{\varepsilon_0 * A * E}{2C} \tag{5}$$

The output waveform of the charge amplifier can be described as a triangular wave that is only depended on the capacitance C. This capacitance is responsible of the gain of the charge amplifier. The resistance R is introduced for stability purposes as it prevents the saturation of the output signal.

III. SENSOR INTERFACE

As mentioned in Section II, the first amplification stage of the interface circuit is the charge amplifier. Two configurations were examined; one for single-ended measurements where a single charge amplifier was employed followed by an inverting amplifier for further amplification and one for differential measurements where two charge amplifiers and a voltage subtractor for extracting the differential signal were employed. For the single-ended measurement, one set of electrodes was utilized, while for the differential measurement both sets of electrodes were used.

Differential measurement eliminates common mode noise, while providing a signal with double the amplitude compared to single-ended configurations. The sensor plates are equally affected from common mode noise, so by subtracting the two signals in a differential measurement, common mode noise picked up by both sets of electrodes can be cancelled [7]. Fig. 3 shows the single ended measurement circuitry that was implemented, while Fig. 4 shows the differential mode.

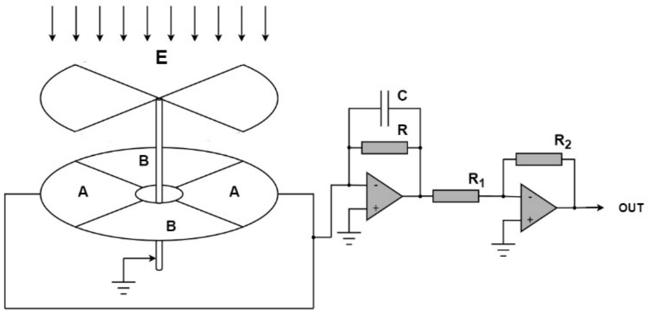

Fig. 3: Field mill sensor with a charge amplifier and an inverting amplifier connected on the output for single ended measurements

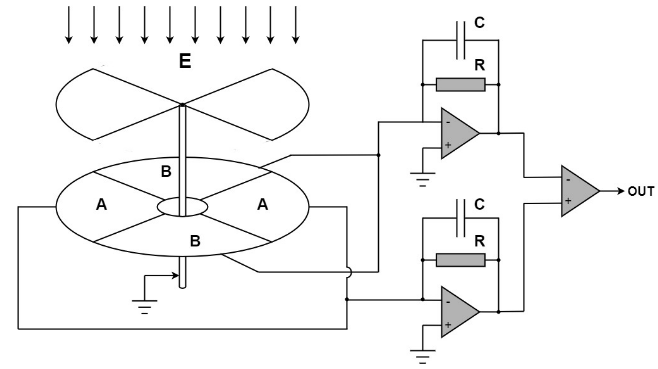

Fig. 4: Field mill sensor with two charge amplifiers connected on both sets of sensing electrodes followed by a subtractor for differential measurements

IV. MEASUREMENTS WITH ARDUINO MICROCONTROLLER

In this study, the Arduino UNO microcontroller was used which is based on the ATmega328p microprocessor, with 14 digital input/output pins, 6 analog pins and a 16 MHz clock frequency. The main hardware part of the Arduino that was utilized is the 10-bit Analog to Digital Converter and the Timer/Counters. The principle of extracting the amplitude of the output signal consists of two measurements. There is one measurement of the output signal every time the sensing electrodes' surface exposure to the field is maximum and a second one after half a rotating period, where the exposure is minimum. This operation happens two times every full rotation and by subtracting these two values the amplitude can be calculated. The polarity of the electric field can be extracted using an optical sensor as there is a 180° phase shift in the output signal every time the polarity changes [8, 9]. This phase shift is presented in Fig. 5 and Fig. 6. An optical sensor mounted on the field mill provides two

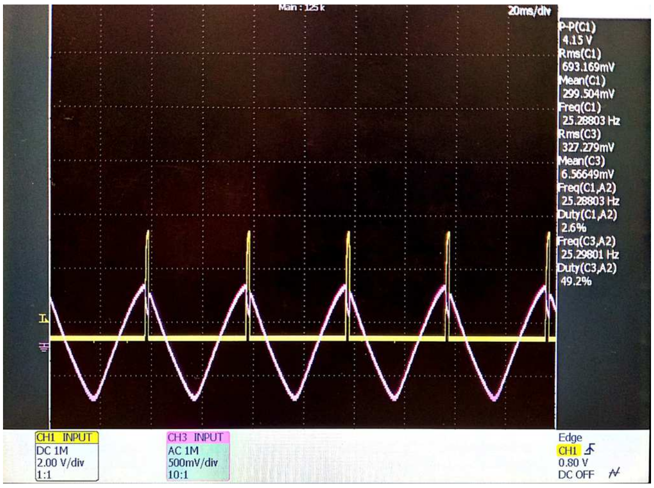

Fig. 5: The triangular wave of the output of the interface circuit in differential mode of operation in relation to the pulse from the optical sensor for negative electric field

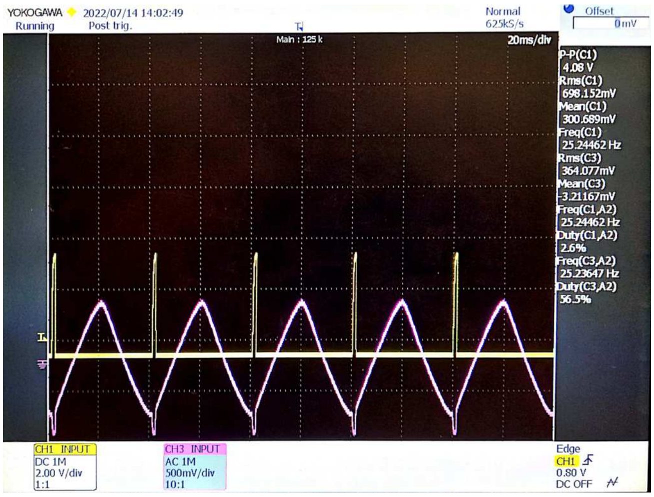

Fig. 6: The triangular wave of the output of the interface circuit in differential mode of operation in relation to the pulse from the optical sensor for positive electric field

pulses in every full rotation, more specifically every time the field mill's sensor area becomes maximum, and it is responsible for the correct timing of the measurements. With the help of an Interrupt Service Routine (ISR) and the Timer Counter 1, an External Interrupt occurs with the rising edge of pin INT0 of the Arduino where the optical sensor is connected. At this moment Arduino saves the measured value of the signal in a variable for later use. A second ISR conducts precisely the second measurement when the Timer1 Overflows at t=T/2. The period of the signal is measured with a third ISR in every cycle so it can be used at the second ISR for better precision. Not only the circuit is independent of the rotational speed but also every slight change in frequency is taken into consideration since there is real time monitoring of the rotational speed. The subtraction of these two measurements gives the amplitude and the polarity of the electric field.

V. Filtering

An analog filter could not be used, as it would introduce a phase difference between the output signal and the signal of the optical sensor, hence the synchronization between them and the extraction of the polarity would be impossible, since the phase difference between the raw signal and the optical sensor signal determines the polarity of the field. To alleviate this problem a digital moving average filter was used, which uses a window (array) to save a number of values in it. With every new value presented to the Arduino input the previous one is discarded, and they all shift a position in the array. After that shift, the average value of the array is calculated which is also the output of this low pass filter. The bigger the window size, the more delay is introduced. This delay doesn't interfere with the synchronization, as is added after the processing and the extraction of the polarity of the field. In other words, the values are processed unfiltered to keep the system synchronized.

VI. Experimental setup

The electric field mill that was used in this study is a 3D printed device, which consists of four sensor plates and two fins connected to the grounded rotor. A constant speed motor turns the grounded rotor. An optical sensor attached to the field mill produces a pulse every time the exposed area is maximized, hence two times in every full rotation (period). This pulse is used for synchronization as described in the previous section.

Fig. 7: 3D printed electric field mill with the parallel plate setup

The measurement setup included a parallel plate setup that provides a constant electric field for experimental and calibration purposes. It consists of two parallel conductive plates with 20 cm distance and a high voltage power supply that can produce four different high voltage values (0-3kV). Therefore, a known electric field is generated, whose polarity can also be controlled by the user. The setup is shown in Fig. 7.

VII. Measurements and results

To illustrate the function of the whole system and to select the best method for the extraction of the electric field values, measurements for different known values of electric field

TABLE I: Capacitance and resistance values of the charge amplifier

Capacitance	Resistance
$C = 1.4\,nF$	$R = 30\,M\Omega$

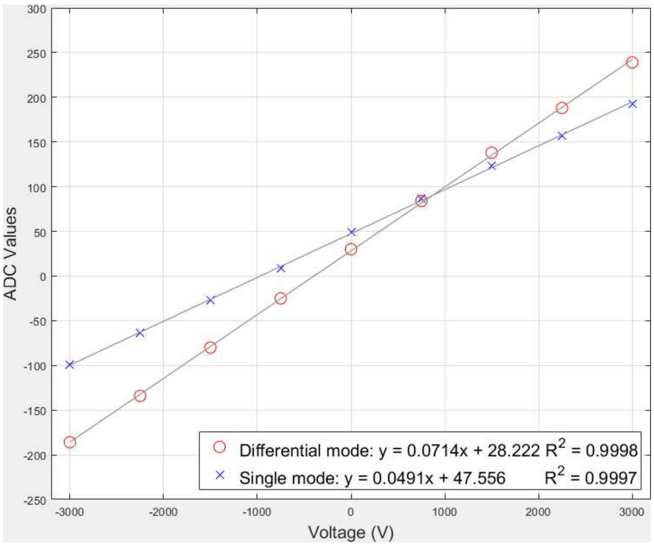

Fig. 8: 10 bit ADC values in relation to the voltage aplied to the parallel plate setup

were acquired. For the single ended measurement, a single charge amplifier was used, and the values of the resistance and the capacitance are presented in Table I. The resistance that was selected provides a current path for the capacitor to be discharged and the main role of the capacitor is to set the gain. There is a dc offset of 0.23 Volts and using the equation $y = 0.0491x + 47.556$ in the Arduino software the electric field can be determined.

The second set of measurements was taken with a differential mode of operation, using two Charge Amplifiers and a subtractor. The values of the capacitance and resistance remained the same. A better fit is obtained with a smaller DC offset (0.14 V). Using the exact same method as described in the previous paragraph the electric field can be determined with the help of the Arduino software. Fig. 8 shows the 10-bit ADC values extracted from the Arduino in relation to the voltage applied to the parallel plates for both modes of operation. Fig. 9 presents the circuit with the Arduino connected and an OLED display providing the ADC values of the electric field before the calibration.

VIII. Conclusion

In this paper, an electric field mill interface circuit, which is capable of monitoring in real time atmospheric electric fields from -15 kV/m up to 15 kV/m, was studied, designed, and successfully tested. The two different circuitry approaches, a single ended and a differential one, provided useful information and through that is clarified that the differential measurement has better linearity, lower noise and lower DC offset. With the utilization of the Arduino microcontroller the electric field and its polarity can be extracted without any further circuitry and analog filters. An OLED screen provided the electric field values to the user. Future adjustments including the integration of the amplification circuit to the body of the 3D printed electric field mill or the utilization of a better and lower power microcontroller could improve the characteristics of it.

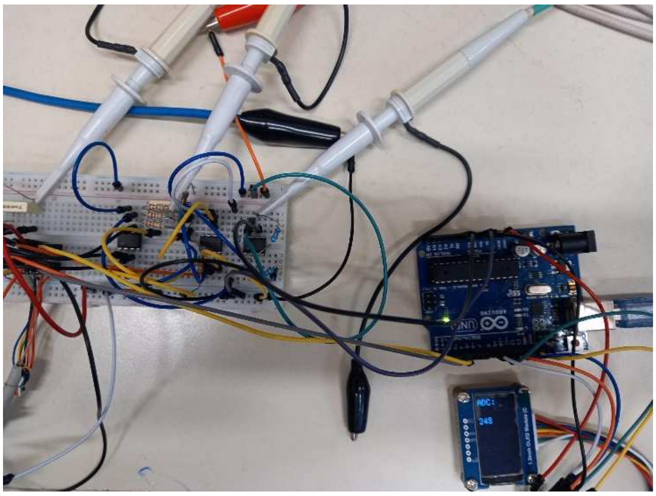

Fig. 9: Complete interface circuit

Acknowledgment

This research has been co-financed by the European Regional Development Fund of the European Union and Greek national funds through the Operational Program Competitiveness, Entrepreneurship and Innovation, under the call RESEARCH – CREATE – INNOVATE (project code: T1EDK-00350).

References

[1] M. A. B. Sidik, et al., "Development of Wireless Electric Field Mill for Atmospheric Electric Field Observation", TELKOMNIKA (Telecommunication Computing Electronics and Control), vol. 12, pp. 1113-1122, 2014

[2] H. Shahroom, Z. Buntat, M. A. B. Sidik, Z. Nawawi and M. I. Jambak, "Atmospheric electric field measurement advances in Southern peninsular Malaysia", 2015 IEEE Conference on Energy Conversion (CENCON), 2015, pp. 116-121, doi: 10.1109/CENCON.2015.7409524.

[3] Y. S. Kim, J. J. Park, "Output Voltage Characteristics of HVDC Electric Field Mill Sensor for Different Speed Variables of Rotating Electrode", Journal of Electrical Engeneering and Technology, 2017, doi: 10.5370/JEET.2017.12.5.2001

[4] Y. Cui, H. Yuan, X. Song, L. Zhao, Y. Liu and L. Lin, "Model, Design, and Testing of Field Mill Sensors for Measuring Electric Fields Under High-Voltage Direct-Current Power Lines", in IEEE Transactions on Industrial Electronics, vol. 65, no. 1, pp. 608-615, Jan. 2018, doi: 10.1109/TIE.2017.2719618.

[5] S. Kamajaya, A. P. Nurmansah and S. Hidayat, "Design, implemetation and calibration of electric field mill", 2016 3rd Conference on Power Engineering and Renewable Energy (ICPERE), 2016, pp. 185-189, doi: 10.1109/ICPERE.2016.7904866

[6] P. Tant, B. Bolsens, T. Sels, D. Van Dommelen, J. Driesen and R. Belmans, "Design and Application of a Field Mill as a High-Voltage DC Meter", in IEEE Transactions on Instrumentation and Measurement, vol. 56, no. 4, pp. 1459-1464, Aug. 2007, doi: 10.1109/TIM.2007.900157.

[7] Graeme J. Marlton R. Giles Harrison, "Fair weather electric field meter for atmospheric science platforms", Journal of Electrostatics, vol. 107, no. 103489, September 2020.

[8] P.E. Secker, "The desing of simple instruments for measurement of charge on insulating surfaces", Journal of Electrostatics, Volume 1, Issue 1, 1975, Pages 27-36, ISSN 0304-3886

[9] D. Yeboah-Amankwah, P. Van Der Made, "Sign discriminating field mill", Journal of Atmospheric and Terrestrial Physics, Volume 54, Issues 7–8, 1992, Pages 851-861, ISSN 0021-9169, https://doi.org/10.1016/0021-9169(92)90052-M.